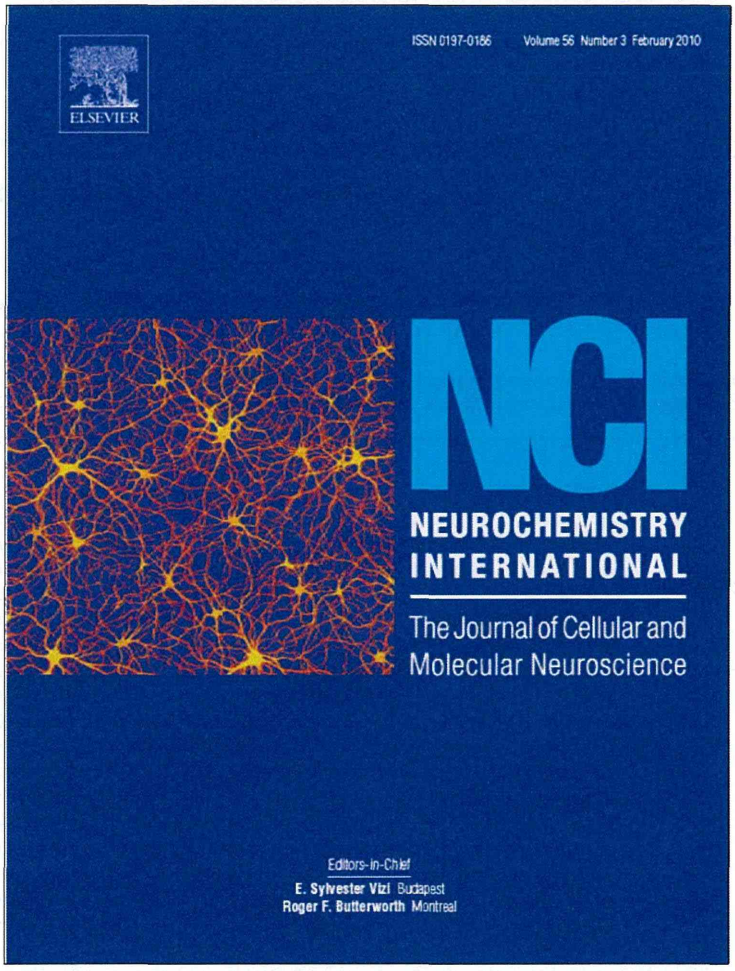

Neurochemistry International 56 (2010) 487–494

Contents lists available at ScienceDirect

Neurochemistry International

journal homepage: www.elsevier.com/locate/neuint

Enhanced expression of C/EBP homologous protein (CHOP) precedes degeneration of fibrocytes in the lateral wall after acute cochlear mitochondrial dysfunction induced by 3-nitropropionic acid

Yoshiaki Fujinami [a], Hideki Mutai [a], Kazusaku Kamiya [a], Kunio Mizutari [a], Masato Fujii [b], Tatsuo Matsunaga [a,*]

[a] Laboratory of Auditory Disorders, National Institute of Sensory Organs, National Tokyo Medical Center, 2-5-1 Higashigaoka, Meguro-ku, Tokyo 152-8902, Japan
[b] Division of Hearing and Balance Research, National Institute of Sensory Organs, National Tokyo Medical Center, Meguro-ku, Tokyo 152-8902, Japan

ARTICLE INFO

Article history:
Received 28 September 2009
Received in revised form 28 November 2009
Accepted 14 December 2009
Available online 21 December 2009

Keywords:
Cochlea
Mitochondria
Apoptosis
Endoplasmic reticulum stress
Oxidative stress

ABSTRACT

We previously reported that treatment of the rat cochlea with a mitochondrial toxin, 3-nitropropionic acid (3-NP), causes temporary to permanent hearing loss depending on the amount of the drug. Furthermore, apoptosis of cochlear lateral wall fibrocytes, which are important for maintaining the endolymph, is a predominant pathological feature in this animal model. 3-NP is known to induce oxidative stress as well as neuronal apoptosis. C/EBP homologous protein gene (*chop*) is one of the marker genes induced during endoplasmic reticulum (ER) stress, and is also considered to be involved in apoptosis. To elucidate the molecular mechanism of cochlear fibrocyte apoptosis induced by 3-NP, we studied spatiotemporal expression of C/EBP homologous protein (CHOP) and other signaling molecules related to ER stress as well as the appearance of apoptotic cells in the cochlear lateral wall after 3-NP treatment. Quantitative real-time PCR revealed that *chop* and activating transcription factor 4 gene (*atf-4*) showed marked increase within 6 h, whereas expression of other ER stress-responsive genes such as *grp78* and *grp94* did not change. Immunohistochemistry showed that 3-NP treatment caused up-regulation of CHOP, especially in type II and type IV fibrocytes, followed by the appearance of terminal deoxynucleotidyl transferase mediated dUTP nick end-labeling (TUNEL)-positive apoptotic cells in the same confined area. Thus, apoptosis of lateral wall fibrocytes induced by 3-NP is likely to be mediated by induction of CHOP. These results contribute clarification of pathological mechanism of cochlear fibrocytes and may lead to development of novel therapeutic strategy for hearing loss.

1. Introduction

Recent advances in auditory research have helped build strategies to cure hearing loss by sensory cell regeneration or prevention of sensory cell loss (Holley, 2005; Kelley, 2006). Most experimental animal models of auditory disorders indicate that noise-induced, hereditary, and drug-induced hearing loss is caused by degeneration of the sensory hair cells or spiral ganglion cells. Recently, several studies reported the involvement of fibrocytes degeneration in the cochlear lateral wall (LW) in hereditary hearing loss (Minowa et al., 1999; Delprat et al., 2005), age-related hearing loss (Spicer and Schulte, 2002), and noise-induced hearing loss (Wang et al., 2002), implying that these non-sensory cells also play important roles in hearing.

We recently established an animal model of acute hearing loss, which is primarily caused by degeneration of LW fibrocytes, using the mitochondrial toxin 3-nitropropionic acid (3-NP) (Hoya et al., 2004; Okamoto et al., 2005; Kamiya et al., 2007; Mizutari et al., 2008). In this model, only less than a 2-fold difference in 3-NP dose differentiates between temporary and irreversible hearing loss. Appearance of TUNEL positive cells (Kamiya et al., 2007; Mizutari et al., 2008), and blockade of fibrocyte degeneration by caspase inhibitor (Mizutari et al., 2008) indicate that degeneration of LW fibrocytes is mainly apoptosis in this model. LW fibrocytes are critical for maintaining the ion concentration of the endolymph by K^+ recycling from the perilymph (Schulte and Steel, 1994; Spicer and Schulte, 1998); and disturbance of the endolymphatic ion concentration leads to immediate hearing loss. Fibrocytes of the LW are divided into five cell types based on structural features, immunostaining patterns and general location (Schulte and Adams, 1989; Spicer and Schulte, 1996; Mutai et al., 2009). Type II and type IV fibrocytes contain numerous mitochondria, and endoplasmic

* Corresponding author. Tel.: +81 3 3411 0111; fax: +81 3 3411 0185.
E-mail address: matsunagatatsuo@kankakuki.go.jp (T. Matsunaga).

0197-0186/$ – see front matter © 2009 Elsevier Ltd. All rights reserved.
doi:10.1016/j.neuint.2009.12.008

reticulum (ER) expresses various types of ion transporters, channels, and pumps, and have significant roles in maintenance of the endolymph. 3-NP is considered to elicit acute deafness by depleting energy in the cochlea, which primarily induces apoptosis of type II and type IV fibrocytes followed by perturbation of endolymph homeostasis. Understanding the molecular pathway of LW fibrocytes cell death is likely to provide insight for preventing auditory disorders caused by LW fibrocyte dysfunction.

3-NP administration alters gene expression in various tissues and induces apoptosis in neuronal cells (Behrens et al., 1995; Pang and Geddes, 1997; Sato et al., 1997). C/EBP homologous protein (CHOP) is a DNA binding protein targeted by activating transcription factor 4 (ATF-4). *chop* (encoding CHOP) is one of the marker genes induced in ER stress (Oyadomari and Mori, 2004), which was originally defined as a cellular response against accumulation of unfolded proteins in the ER (Xu et al., 2005). In addition, the accumulation of unfolded proteins in mitochondria also induces CHOP expression (Zhao et al., 2002). CHOP is considered to be involved in apoptosis in various cell types (Matsumoto et al., 1996; Maytin et al., 2001). Part of the downstream pathways of CHOP that leads to apoptosis was recently revealed. It was reported that overexpression of Bcl-2 blocks CHOP-induced apoptosis (Matsumoto et al., 1996), Tribbles-related protein 3 (TRB3) repress the transcriptional activity of CHOP (Ohoka et al., 2005) and Bcl-2 interacting mediator of cell death (Bim) is closely related to the CHOP-induced apoptosis (Puthalakath et al., 2007). CHOP expression is induced in Parkinson's disease (Holtz and O'Malley, 2003), ischemia–reperfusion injury (Tajiri et al., 2004), and diabetes (Araki et al., 2003). The linkage between CHOP induction and cell death raises the possibility that CHOP may also play a role in eliciting apoptosis of LW fibrocytes exposed to 3-NP. To explore this possibility, we examined the induction of CHOP and other ER stress-related molecules such as *atf-4* gene (encoding an ATF-4) in the LW of 3-NP-treated animals, and the relationship of CHOP expression and apoptosis in the degenerating cells.

2. Results

2.1. Time course of hearing after 3-NP treatment

The time course of hearing in rats treated with 3-NP was measured by auditory brainstem response (ABR). Because our previous studies using the same animal model as the present study showed a remarkable difference in the time course of ABR thresholds at 8 kHz and 20 kHz between TTS and PTS rats, we measured ABR thresholds at these two frequencies in the present study. The rats treated with 300 mM 3-NP demonstrated severe hearing loss at both 8 kHz and 20 kHz (72.0 ± 5.9 dB and 85.5 ± 1.5 dB, respectively) 1 day after the treatment (DAT, Fig. 1). At 7 DAT, the threshold shift at 8 kHz recovered to almost the normal range (15.0 ± 1.2 dB) and the threshold shift at 20 kHz gradually recovered to a moderate level of hearing loss (40.0 ± 8.9 dB). These rats were referred as temporary threshold shift (TTS) rats. In contrast, the ABR threshold in rats treated with 500 mM 3-NP exceeded the highest measurable level at both tested frequencies 3 h after the treatment and did not show any signs of recovery even at 7 DAT. These rats were referred as permanent threshold shift (PTS) rats. Saline-treated rats maintained normal thresholds, indicating that the surgical procedures did not cause hearing loss. These phenotypes were consistent with our previous data (Hoya et al., 2004).

2.2. Time course of chop and atf-4 expression in the LW after 3-NP treatment

To explore the molecular events during hearing loss by 3-NP, we investigated whether the genes activated during ER stress were

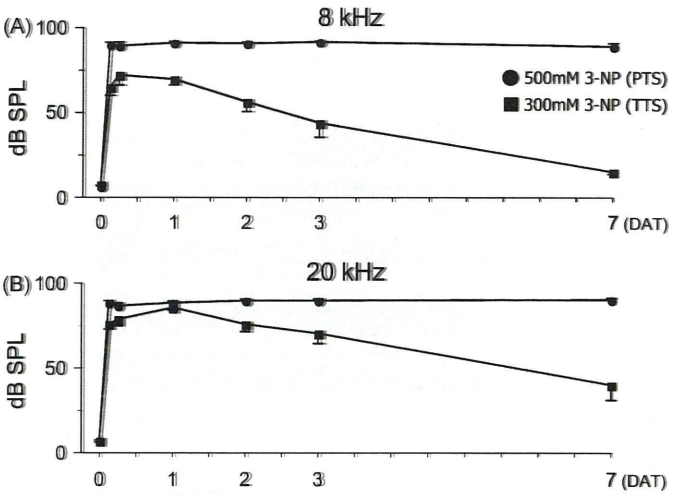

Fig. 1. Time course of auditory thresholds in temporary threshold shift (TTS) rats treated with 300 mM 3-nitropropionic acid (3-NP) and permanent threshold shift (PTS) rats treated with 500 mM 3-NP. The threshold shifts were recorded at 8 kHz (A) and 20 kHz (B). Although the thresholds reached their peak at 1 day after 3-NP treatment (DAT) and then decreased in the TTS rats, the thresholds in the PTS rats exceeded the measurable levels at 3 h after the treatment and were stable at 7 DAT. $n = 5$.

up-regulated in the LW after 3-NP treatment. Expression of four ER stress-responsive genes (*chop*, *atf-4*, *grp78*, and *grp94*) along with the housekeeping gene glyceraldehyde-3-phosphate dehydrogenase (*gapdh*) in the cochlear middle turn of TTS and PTS rats was measured using semi-quantitative reverse transcription PCR (RT-PCR). LW of cochlear middle turn was chosen because histological changes indicating degeneration of LW fibrocytes were evidently detected at this region in both TTS and PTS rats and there was a remarkable difference in the time course of ABR thresholds at this region between TTS and PTS rats.

We found that all five transcripts were successfully amplified in the LW from untreated rats (Fig. 2A). In addition, two of them, *chop* and its activator *atf-4*, both of which are suggested to be involved in activation of the apoptotic pathway, were up-regulated after 3-NP treatment. The changes in *chop* and *atf-4* expression from 3 h to 7 DAT were similar in the TTS and PTS rats; an increase of the PCR bands occurred in TTS and PTS rats within a few hours after treatment, but these band intensities dropped to the untreated levels in TTS rats and even lower in PTS rats at 1 DAT. In contrast, expression of *grp78* and *grp94*, molecular chaperones in the ER lumen and indicators of cell survival (Kaufman, 1999), did not show apparent changes throughout the experimental period (Fig. 2A), indicating that not all the genes mediating ER stress are stimulated in the LW after 3-NP treatment.

In the next experiment, expression levels of *chop* and *atf-4* after 3-NP treatment from which the changes were seen in the RT-PCR results were further evaluated by quantitative real-time RT-PCR (qPCR). These gene expressions were compared with those in untreated rats (0 DAT, $n = 5$). Because neither *grp78* nor *grp94* expression did not change in the screening by RT-PCR, these gene expressions were not measured by qPCR. The level of *chop* (Fig. 2B) was increased at 6 h after the treatment (390 ± 91% in TTS rats, $p < 0.05$, and 595 ± 262% in PTS rats), confirming our previous observation that *chop* is induced promptly after 3-NP treatment. However, no significant difference in the peak level of *chop* was observed between PTS and TTS rats. At 1 DAT, the *chop* level dropped sharply to 53 ± 6% in TTS rats and 58 ± 16% in PTS rats, followed by gradual recovery to the untreated level in TTS and PTS rats until 7 DAT. As observed for *chop*, *atf-4* expression significantly increased and reached its peak 6 h after 3-NP treatment (Fig. 2C). The increase in *atf-4* expression was lower than that in *chop* both in TTS rats

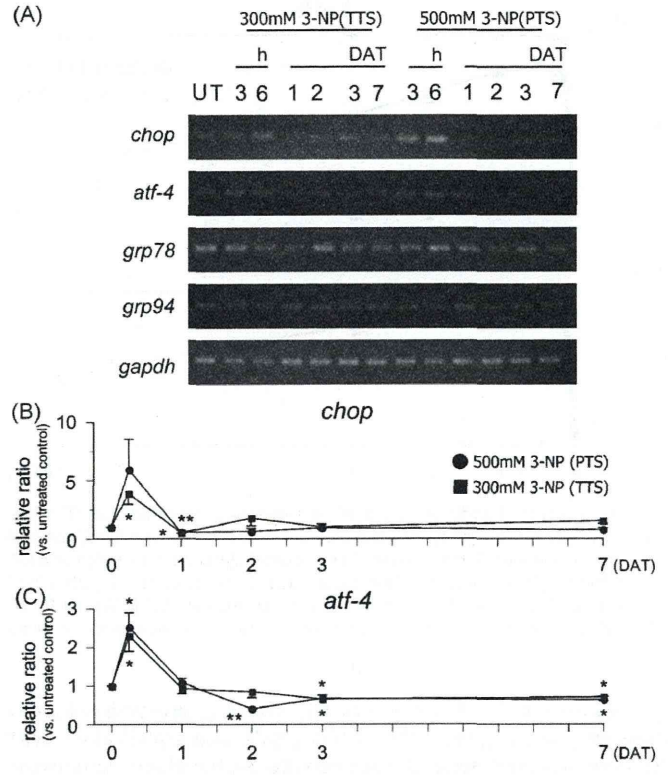

Fig. 2. Expression of ER stress-responsive genes in the lateral wall (LW) after 3-NP treatment. Expression was determined by semi-quantitative reverse transcription PCR (A) and quantitative real-time PCR (B and C). UT; untreated control rats; *gapdh*; glyceraldehyde-3-phosphate dehydrogenase. DAT; day(s) after 3-NP treatment. *chop* (B) and *atf-4* (C) were temporarily induced in the LW 6 h after treatment in both TTS rats treated with 300 mM 3-NP and PTS rats treated with 500 mM 3-NP. *chop* was decreased to approximately half of the untreated level (0 h) at 1 DAT and then recovered to the normal level. $n = 5$. $^{*}p < 0.05$, $^{**}p < 0.01$, significant difference vs. untreated control.

(230 ± 40%, $p < 0.05$) and in PTS rats (252 ± 38%, $p < 0.05$). In the TTS and PTS rats, *atf-4* was down-regulated to 71 ± 10% and 64 ± 8% of the untreated level, respectively, at 7 DAT. Taken together, *chop* and *atf-4*, which are activated by various stimuli including ER stress, were responsive to 3-NP in the present study, whereas expression of the other candidate genes, *grp78* and *grp94*, did not change in response to the treatment.

2.3. Spatial expression patterns of CHOP and apoptosis in the LW after 3-NP treatment

We next investigated spatial expression patterns of the CHOP in the LW after 3-NP treatment. CHOP signals were detected using immunohistochemistry with paraformaldehyde-fixed, paraffin-embedded tissues. We focused on the cochlear middle turn to compare with expression levels of *chop* and *atf-4* by RT-PCR and qPCR. The same primary antibody for CHOP was used in this study as that used for a previous report (Hayashi et al., 2005). To ascertain specific binding of the primary antibody, a set of sections was stained in a similar way without the primary antibody, and the staining was not detected (data not shown). Types of LW fibrocytes were judged based on their localization within the spiral ligament according to the previous studies (Schulte and Adams, 1989; Spicer and Schulte, 1996; Mutai et al., 2009). Fig. 3 shows distribution of the CHOP signal at the middle turn of the LW before and after 3-NP treatment. CHOP was detected at low levels in the LW of untreated and saline-treated rats (Fig. 3A and F). The low CHOP signal level persisted until 6 h after treatment in both TTS and PTS rats (Fig. 3B and G). The CHOP signal intensity started to increase over the entire spiral ligament at 1 DAT in both TTS and PTS rats (Fig. 3C and H), with the most intense staining in the area of type II and type IV fibrocytes in PTS rats. At this time in the TTS, CHOP immunoreactivity was localized mainly in the cytoplasm (Fig. 3C and L), and localized slightly also in the nuclei. CHOP immunoreactivity did not remain in the LW at 2 DAT (Fig. 3D). On the other hand, immunoreactivity in the PTS rats at 1 DAT was localized mainly in the nuclei (Fig. 3H and N), and remained in the LW at 2DAT and 3 DAT (Fig. 3I and J). Fibrocyte degeneration was not apparent in the spiral ligament of either TTS or PTS rats until 1 DAT. In TTS rats, fibrocyte degeneration which was indicated by a region free of cellular nuclei was observed in the area of type II and type IV fibrocytes at 2 DAT (Fig. 3D and M) and 3 DAT (Fig. 3E) and area of fibrocyte degeneration did not expand from 2 DAT to 3 DAT. In PTS rats, a subpopulation of type II and type IV fibrocytes started to disappear and CHOP immunoreactivity was detected around this area at 2 DAT (Fig. 3I and O), and a majority of the fibrocytes in the LW had degenerated at 3 DAT (Fig. 3J).

Because our previous study showed that death of LW fibrocytes is mediated by an apoptotic pathway (Kamiya et al., 2007; Mizutari et al., 2008), we next investigated whether the onset of apoptotic cell death coincides with the onset of CHOP induction. The paraffin sections were used for the terminal deoxynucleotidyl transferase mediated dUTP nick end-labeling (TUNEL) assay, a method generally accepted to detect DNA fragmentation caused by activation of apoptotic pathways (Fig. 4). TUNEL-positive cells were not detected in untreated and saline-treated LWs (Fig. 4A and F). In TTS rats (Fig. 4B–E), TUNEL-positive cells appeared at 2 DAT in the area of type II fibrocytes (Fig. 4D and M). A small number of TUNEL-positive cells were also evident at 3 DAT (Fig. 4E). In PTS rats (Fig. 4G–J), TUNEL-positive cells were detectable as early as 1 DAT in the type II/IV fibrocytes (Fig. 4H). The number of TUNEL-positive cells in the LW gradually increased from 1 to 3 DAT (Fig. 4H–J). To clarify whether CHOP induction and apoptotic cell death are associated, the LWs in the untreated or PTS rats were subjected to a double immunofluorescence study (Fig. 5A–J). CHOP signal (red) was low in untreated rats (Fig. 5A, D, E) and intensified in the area of type II and type IV fibrocytes at 1 DAT in PTS rats (Fig. 5F, I, and J). TUNEL-positive apoptotic cells (green) were undetectable in the LW of untreated rats (Fig. 5B, D, and E) but were observed in PTS rats at 1 DAT (Fig. 5G, I, and J). Although apoptotic cells were not convincingly co-immunostained with CHOP in PTS rats at 1 DAT, they were confined to the CHOP-positive area (Fig. 5I and J). In untreated rats, the CHOP signal visualized by fluorescein staining in the stria vascularis (Fig. 5A) was inconsistent with the absence of a signal in the stria vascularis by 3,3′-diaminobenzidine (DAB) staining (Fig. 3A). The difference was considered to be due to the methods used for antigen retrieval. Because apoptotic cells were not detected in the stria vascularis, we focused on the CHOP expression in the spiral ligament. Thus, CHOP expression in the stria vascularis is not discussed further in this study. Overall, we demonstrated that induction of the CHOP signal was followed by apoptotic cell death in the LW fibrocytes after 3-NP treatment.

3. Discussion

In this study, we examined the time course of CHOP expression, apoptosis, and degeneration of fibrocytes after administration of 3-NP. We demonstrated temporary CHOP expression in the confined area of LW in which fibrocyte degeneration occurred afterwards. In TTS rats, TUNEL-positive cells became detectable at 2 DAT, approximately 1 day after CHOP induction. In PTS rats, a few TUNEL-positive cells were detectable at 1 DAT, when the CHOP level was first up-regulated. Then, the number of TUNEL-positive cells increased significantly at 2 DAT. CHOP and TUNEL signals are detectable in the same area, but co-localization of these two

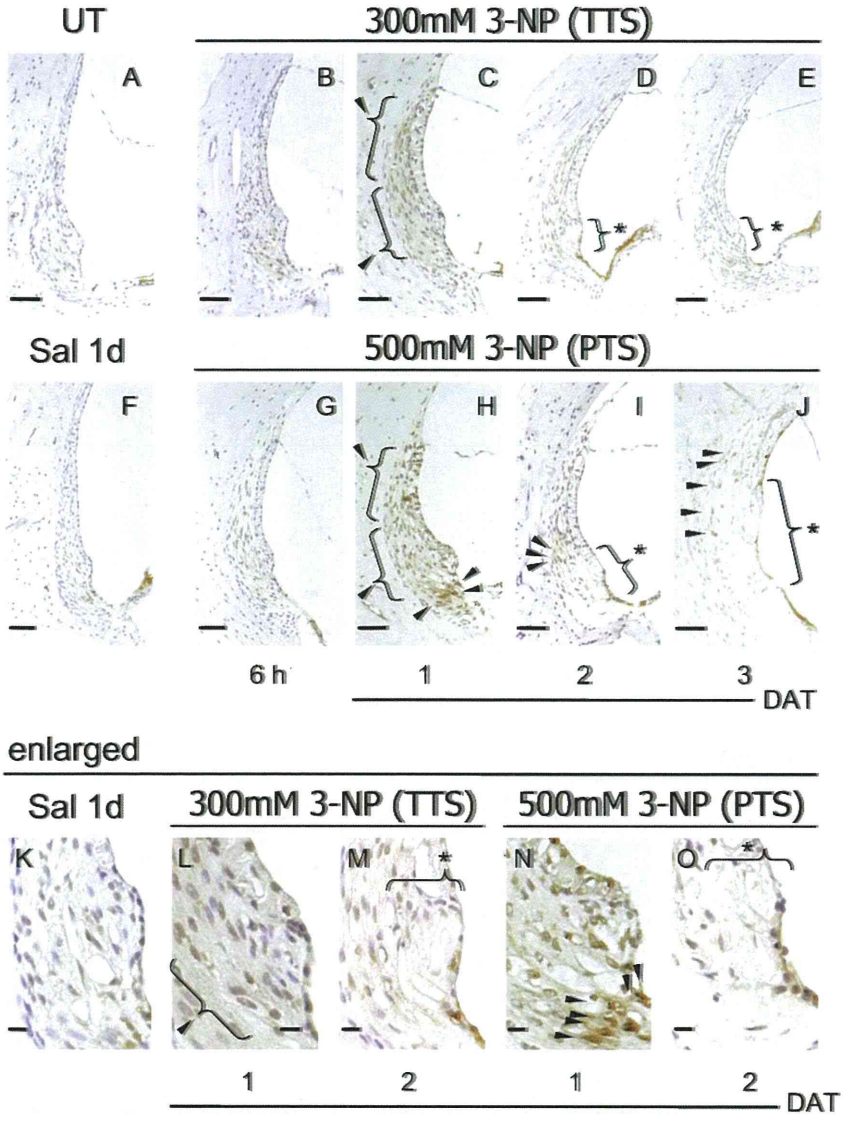

Fig. 3. Immunohistochemical analysis of CHOP expression in the LW after 3-NP treatment. In untreated control rats (UT), a low level of CHOP was detectable in the entire LW (A). In TTS rats treated with 300 mM 3-NP (B–E, L, and M), the CHOP signal (arrowheads) was unchanged at 6 h but intensified 1 day after 3-NP treatment (DAT) (C) compared with saline-treated rats (Sal 1d, F, K). A limited area (asterisk) of the LW had degenerated at 2 DAT and 3 DAT (D, E). In PTS rats treated with 500 mM 3-NP (G–J, N, and O), an intense CHOP signal (arrowheads) was evident, especially in the area of type II and type IV fibrocytes of the LW at 1 DAT (H). At 2 DAT, type II and type IV fibrocytes appeared to start degeneration (asterisk) (I), and the area of degenerated fibrocytes expanded at 3 DAT (J). K–O are enlarged images of spiral prominence of F, C, D, H and I, respectively. Scale bar = 50 μm (A–J) and 10 μm (K–O).

staining was not detected. Because CHOP is known to be involved in inducing apoptosis (Matsumoto et al., 1996; Maytin et al., 2001), we speculate that the delay of TUNEL appearance is due to signal transduction for apoptotic pathways. Tajiri et al. (2004) reported that *chop* induction in the striatum peaks 12 h after the occlusion of the carotid artery, followed by detection of numerous TUNEL-positive cells at 24 h. Investigation of signaling molecules downstream of CHOP (Wang et al., 1998; Sok et al., 1999) and activation of pro-apoptotic molecules such as caspases after 3-NP treatment may clarify the direct association of CHOP activation with apoptotic cell death in LW fibrocytes. In the present study, of note is that nuclei were also positively stained for CHOP in PTS rats at 1 DAT, which is required to exert functional effect for this transcription factor (Zinszner et al., 1998).

The activation of ATF-4 and CHOP in the LW of 3-NP-treated rats is reminiscent of CHOP and ATF-4 activation in ischemic brain (Hayashi et al., 2005). Induction of the same molecules in these two affected areas is probably caused by the features of energy depletion which are shared by mitochondrial dysfunction and ischemia. What is the mechanism of the expression of *atf-4* and CHOP which is the downstream target of ATF-4 in LW fibrocytes? The mitochondrial toxin 3-NP is an irreversible inhibitor of succinate dehydrogenase (complex II of the electron transport chain) (Coles et al., 1979). Inhibition of energy metabolism by 3-NP results in the production of reactive oxygen species (Beal et al., 1995; Lee et al., 2002; Rosenstock et al., 2004) that causes oxidative stress and neuronal cell death (Behrens et al., 1995; Pang and Geddes, 1997; Sato et al., 1997; Higuchi, 2004). Oxidative stress induces ER stress (Yu et al., 1999), and this is known to enhance CHOP expression (Oyadomari and Mori, 2004). In addition, cells exposed to 3-NP also release mitochondrial Ca^{2+}, which is caused by an increasing amount of reactive oxygen species (Rosenstock et al., 2004) and rapid elevation of the intracellular Ca^{2+} level is known to enhance CHOP expression (Deshpande et al., 1997; Tanaka et al., 2005). Thus, oxidative stress, ER stress and increase in the intracellular Ca^{2+} level are related events in terms of the molecular signalling pathways. We assume 3-NP induced ATF-4 and CHOP in LW by these mechanism.

Our findings are not in full agreement with the hypothesis that CHOP is activated exclusively in response to ER stress in the LW

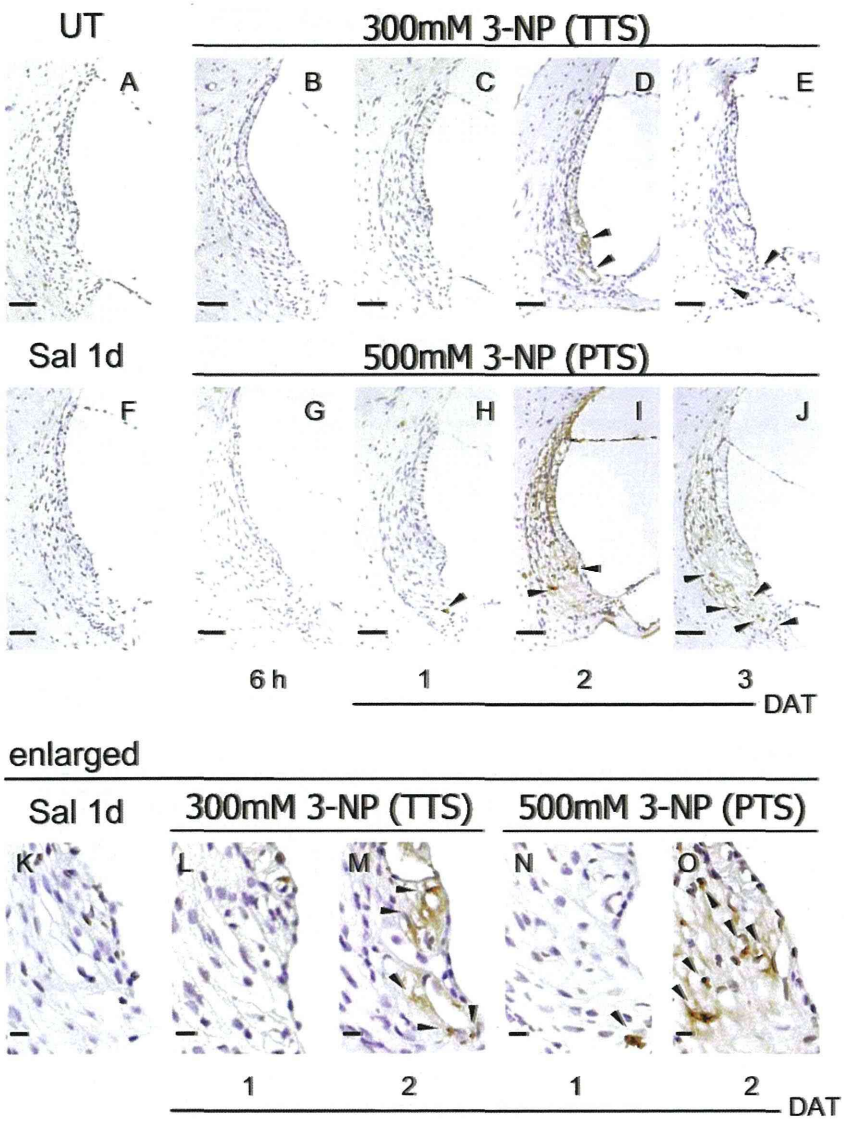

Fig. 4. TUNEL histochemical analysis of apoptotic cells in the LW after 3-NP treatment. Apoptotic cells were not detected in untreated control rats (UT; A) or in saline-treated rats (Sal 1d; F). In TTS rats treated with 300 mM 3-NP (B–E), a small number of apoptotic cells (arrowheads) were found at 2 DAT and 3 DAT (D, E). In PTS rats treated with 500 mM 3-NP (G–J), apoptotic cells were detectable at 1 DAT (H). The number of apoptotic cells (arrowheads) increased as the degenerating area expanded at 2 DAT and 3 DAT (I, J). K–O are enlarged images of spiral prominence of F, C, D, H and I, respectively. Scale bar = 50 μm (A–J) and 10 μm (K–O).

treated with 3-NP, because multiple attempts failed to show significant up-regulation of the ER stress mediators *grp78* and *grp94*. These results suggest that either a partial ER stress-response pathway including ATF-4 and CHOP is activated, or that mechanisms other than ER stress are responsible for the activation of the two molecules in the LW treated with 3-NP. CHOP has been reported to be induced without activation of other ER stress-responsive proteins such as GRP78 in a cultural experimental model of mitochondrial stress (Zhao et al., 2002). In this model, accumulation of unfolded proteins in the mitochondria resulted in induction of CHOP and mitochondrial molecular chaperones (e.g., Cpn60, Cpn10 and mtDnaJ), but did not induce non-mitochondrial chaperones including GRP78. Moisoi et al. (2009) also reported that *chop* expression was increased by mitochondrial dysfunction in the brain. Similarly, induction of *atf-4* and *chop* in the LW after 3-NP treatment may also be caused by mitochondrial stress following oxidative stress. On the other hand, investigation of PERK, IRE-1 and ATF-6 is necessary to demonstrate that ER stress is concerned with the increase of *chop* expression in this study.

The expression levels of *chop* at 6 h after 3-NP treatment and at 1 DAT were not significantly different between TTS and PTS rats, despite the contrasting number of degenerating cells at 3 DAT. Immunohistochemical study revealed nuclear staining of CHOP, which is required to undergo functional role for transcription factor, in PTS rats but rarely in TTS rats. This may explain the different levels of apoptosis at 3 DAT. Another possibility is that CHOP may be involved in the only initial induction of apoptosis in this model and another death pathway which sustained ongoing cell death was also activated in PTS rats but not activated in TTS rats. Further study to identify regulators of degeneration in LW fibrocytes will provide us with insight to develop strategies to prevent death of LW fibrocytes.

In summary, we characterized a novel molecular mechanism of acute hearing loss caused by 3-NP administration and identified CHOP, a mediator of oxidative stress, ER stress, and mitochondrial stress, as a preceding marker of damage in LW fibrocytes.

4. Experimental procedures

4.1. Animals and drug administration

Male Sprague–Dawley rats (6–8 weeks old, weighing 170–230 g) were used. The rats were housed in metallic breeding cages in a room with a light/dark

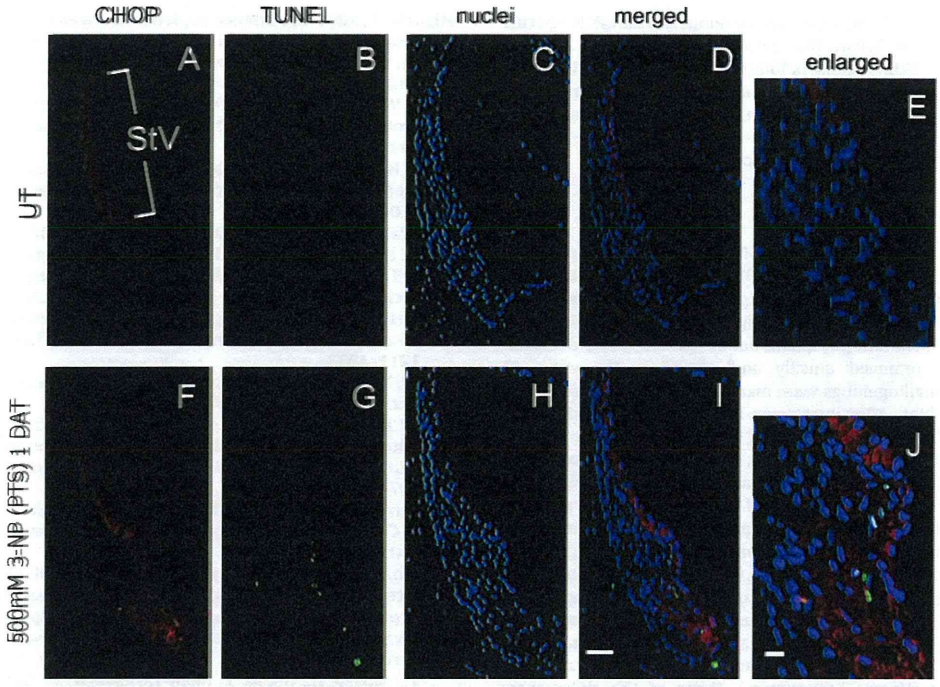

Fig. 5. Concurrent detection of CHOP and apoptosis in the LW after 3-NP treatment. The LW of untreated control rats (UT; A–E) and PTS rats treated with 500 mM 3-NP (F–J) were double-immunostained with antibodies to CHOP (red) and TUNEL (green), and counterstained with DAPI for nuclear staining (blue). Although apoptotic cells were not observed in untreated rats (B, D, and E), apoptosis was detected in the area of type II and type IV fibrocytes in PTS rats 1 day after 3-NP treatment (PTS rats 1 DAT; G) where the CHOP signal was enhanced (F, I, J). E and J were enlarged images of spiral prominence of D and H, respectively. StV; stria vascularis. Scale bar = 50 μm (A–D, F–I) and 10 μm (E, J). (For interpretation of the references to color in this figure legend, the reader is referred to the web version of the article.)

Table 1
PCR primers and their target genes used in the study.

Gene	Acc. number	Sequence (5′ > 3′)		Product length (bp)	Annealing temperature (°C)
		Forward	Reverse		
chop	U30186	AGTCTCTGCCTTTCGCCTTT	GCCACTTTCCTCTCATTCTC	382	55.4
atf-4	NM_024403	GCTGCCCCCTTTACATTCTT	AGCACAAAGCACCTGACTAC	615	54.5
grp78	XM_213908	AACGACCCCTGACAAAAGAC	TAGCCAATTCCTCCTCTCCC	768	57.9
grp94	XM_343192	ACACGGCTTGCTAAACTTCT	CTCTGGCTCTTCCTCTACCT	771	54.2
gapdh	M17701	GCCAAAAGGGTCATCATCTC	GCCTCTCTCTTGCTCTCAGT	715	55.5

Abbreviations: Acc. number: accession number; *chop*: C/EBP homologous protein; *atf-4*: activating transcription factor-4; *grp78* and *grp94*: glucose-regulated protein 78 and 94; *gapdh*: glyceraldehyde-3-phosphate dehydrogenase.

cycle of 12 h and humidity of 55% at 23 °C, with free access to food and water for at least 7 days before use. In these rats, hearing loss was induced by surgical administration of different concentrations of 3-NP onto the inner ear (Hoya et al., 2004). Before surgery, the rats were anesthetized with pentobarbital (40–50 mg/kg, i.p.) or pentobarbital (20–25 mg/kg, i.p.), ketamine (40–60 mg/kg, i.p.) and xylazine (4–6 mg/kg, i.p.). An incision was made posterior to the left pinna near the external meatus after local administration of lidocaine (1%). The left otic bulla was opened to approach the round window niche. The tip of a polyethylene tube (PE10, Becton Dickinson & Co., Franklin Lakes, NJ) was drawn to a fine tip in a flame and gently inserted into the round window niche. 3-NP (Sigma, St. Louis, MO) was dissolved in saline at 300 mM or 500 mM and the pH was adjusted to 7.4 with NaOH. Each 3-NP solution (3 μL) was administered with a syringe pump. Following 3-NP treatment, a tiny piece of gelatin was placed on the niche to keep the solution in the niche during head movement after awakening from anesthesia, and the wound was closed (Hoya et al., 2004; Okamoto et al., 2005). All the experimental procedures were performed in accordance with guidelines from the National Tokyo Medical Center, and were approved by the Animal Care and Use Committee of the Institute. Adequate measures were taken to minimize pain or discomfort of experimental animals.

4.2. Measurement of auditory brainstem response

ABRs were recorded from each rat before 3-NP treatment, and 3 h, 6 h, 1, 2, 3 and 7 days after 3-NP treatment. Pure tone bursts of 8 kHz and 20 kHz (0.2 ms rise/fall time 1 ms flat segment) were used, and auditory thresholds in the treated ear were measured at the same time point using incremental steps of 5 dB. Details of ABR recording were previously described (Hoya et al., 2004).

4.3. Semi-quantitative reverse transcription PCR

After the rats were anesthetized from each rat before 3-NP treatment, and 3 h, 6 h, 1, 2, 3 and 7 days after 3-NP treatment ($n = 5$), temporal bones were quickly removed and immersed in RNA later (Takara Bio, Shiga, Japan) on ice, followed by dissection of the middle turn of the LW. Total RNA was isolated using TRIzol reagent (cultural gen, Carlsbad, CA) according to the manufacturer's protocol. Total RNA was extracted by DEPC-treated water and the purity of total RNA was measured with a UV/visible spectrophotometer (Ultrospec 2100 pro; Amersham Pharmacia Biotech, Piscataway, NJ) by the ratio of OD_{260}/OD_{280}. First-strand cDNA synthesis was performed using 100 ng of total RNA and oligo(dT)$_{12-18}$ primers in a total volume of 20 μL according to the SuperScript III RNase H$^-$ Reverse Transcriptase protocol (cultural gen). We used PCR primers specific for *chop*, *atf-4*, glucose-regulated protein *grp78* and *grp94*, and *gapdh*. The sequences of the PCR primers, sizes of the predicted PCR products, and the annealing temperature are listed in Table 1. The target genes were amplified in 25 μL of reaction containing 2.5 μL of diluted cDNA, 0.2 μM of each dNTP, 0.4 μM of each primer, 0.625 U of Taq DNA polymerase (Sigma) and 1× buffer (10 mM Tris–HCl (pH 8.3), 50 mM KCl, 1.5 mM $MgCl_2$ and 0.001% gelatin). PCR was conducted at 94 °C for 5 min, 30 cycles of 94 °C for 1 min, the specific annealing temperature for 1 min, and 72 °C for 2 min, followed by 72 °C for 10 min, and then 10 μL of each PCR product was analyzed by 1% agarose gel electrophoresis in Tris–acetate-EDTA buffer. PCR products were electrophoresed and visualized using ethidium bromide. The images were captured by CS Analyzer (Atto, Tokyo, Japan).

4.4. Quantitative real-time RT-PCR analysis

qPCR was performed according to manufacturer's protocols for the ABI PRISM 7000 Sequence Detection System (Applied Biosystems, Foster City, CA). The

identical cDNAs prepared for RT-PCR were used as the templates for qPCR. Specific primer sets were purchased from Takara Bio. qPCR was performed in 25 μL of reaction mixture containing 1× SYBR Premix Ex Taq (Takara Bio), 1× ROX Reference Dye, 0.2 μM of each primer and cDNA. PCR was conducted for 5 s at 95 °C and 31 s at 60 °C for 40 cycles. Gene expression levels were normalized using *gapdh* as an internal control. Results of ABR and qPCR are expressed as the mean ± standard error, and statistical significance was determined by one sample *t*-test.

4.5. Immunohistochemical analysis

Histological sample were made on the before 3-NP treatment and 1 day after vehicle treatment, and 6 h, 1, 2 and 3 days after 3-NP treatment ($n \geq 3$). Rats were deeply anesthetized with pentobarbital (50 mg/kg, i.p.) and perfused intracardially with 0.01 M sodium phosphate buffer (pH 7.4) containing 8.6% sucrose, followed by 4% paraformaldehyde in 0.1 M sodium phosphate buffer (pH 7.4). After decapitation, temporal bones were removed quickly and placed in the same 4% paraformaldehyde fixative. Small openings were made at the round window, oval window and apex of the cochlea. After immersion in the fixative overnight, the temporal bones were decalcified by placement in 5% EDTA and 4% sucrose in 0.1 M sodium phosphate buffer (pH 7.4) at 4 °C for 2 weeks, dehydrated, and embedded in paraffin. Transverse cochlear sections at 5-μm thickness were cut and mounted on glass slides. After rehydration, sections were treated with 0.3% hydrogen peroxide in methanol to quench peroxidase activity. For epitope retrieval, slides were boiled in citrate buffer (pH 6.0) in a microwave. After blocking nonspecific binding with 1% normal goat serum (Vector Laboratories, Burlingame, CA), the slides were incubated with monoclonal anti-CHOP (Santa Cruz Biotechnology, Santa Cruz, CA) at a 1:100 dilution at 4 °C overnight. The slides were washed and then incubated with biotinylated anti-mouse IgG (Vector Laboratories) at a 1:200 dilution, and the signal was colorized using VECTASTAIN Elite ABC kit (Vector Laboratories) and DAB Substrate kit for Peroxidase (Vector Laboratories). Some of the slides were counterstained with hematoxylin. Some of the unstained sections were processed for TUNEL histochemical staining using ApopTag Peroxidase *In Situ* Apoptosis Detection kit (Chemicon International, Temecula, CA) according to the manufacturer's protocol. The TUNEL reaction mixture was added to each sample in a humidified chamber, followed by incubation for 1 h at 37 °C for colorization with DAB. For fluorescent immunostaining, the sections were incubated with anti-CHOP at a dilution of 1:50. The sections were subsequently treated with proteinase K (DakoCytomation, Carpinteria, CA) and incubated with Alexa Fluor 568 anti-mouse IgG (Molecular Probes, Eugene, OR) at a 1:1000 dilution. Thereafter, the ApopTag Fluorescein Direct *In Situ* Apoptosis Detection kit (Chemicon) was used according to the manufacturer's protocol. The sections were then covered with PermaFluor Aqueous Mounting Medium (Thermo Shandon, Pittsburgh, PA) with DAPI (1 μg/mL; Dojindo, Kumamoto, Japan).

Acknowledgements

This study is supported by a Health Science Research Grant from the Ministry of Health, Labor, and Welfare of Japan (H16-kankakuki-006 to T.M.). The authors would like to thank Ms. Rie Komatsuzaki and Ms. Ritsuko Kusano for their excellent technical support, Dr. Eiji Hashino for critical reading and editing of this manuscript, Drs. Takeshi Iwata, Hiroyuki Ozawa, Seiichi Shinden and Mr. Susumu Nakagawa for their valuable guidance in technical aspects of our experiments.

References

Araki, E., Oyadomari, S., Mori, M., 2003. Impact of endoplasmic reticulum stress pathway on pancreatic beta-cells and diabetes mellitus. Exp. Biol. Med. (Maywood) 228, 1213–1217.

Beal, M.F., Ferrante, R.J., Henshaw, R., Matthews, R.T., Chan, P.H., Kowall, N.W., Epstein, C.J., Schulz, J.B., 1995. 3-Nitropropionic acid neurotoxicity is attenuated in copper/zinc superoxide dismutase transgenic mice. J. Neurochem. 65, 919–922.

Behrens, M.I., Koh, J.J., Canzoniero, L.M., Sensi, S.L., Csernansky, C.A., Choi, D.W., 1995. 3-Nitropropionic acid induces apoptosis in cultured striatal and cortical neurons. Neuroreport 6, 545–548.

Coles, C.J., Edmondson, D.E., Singer, T.P., 1979. Inactivation of succinate dehydrogenase by 3-nitropropionate. J. Biol. Chem. 254, 5161–5167.

Delprat, B., Ruel, J., Guitton, M.J., Hamard, G., Lenoir, M., Pujol, R., Puel, J.L., Brabet, P., Hamel, C.P., 2005. Deafness and cochlear fibrocyte alterations in mice deficient for the inner ear protein otospiralin. Mol. Cell. Biol. 25, 847–853.

Deshpande, S.B., Fukuda, A., Nishino, H., 1997. 3-Nitropropionic acid increases the intracellular Ca^{2+} in cultured astrocytes by reverse operation of the Na^+–Ca^{2+} exchanger. Exp. Neurol. 145, 38–45.

Hayashi, T., Saito, A., Okuno, S., Ferrand-Drake, M., Dodd, R.L., Chan, P.H., 2005. Damage to the endoplasmic reticulum and activation of apoptotic machinery by oxidative stress in ischemic neurons. J. Cereb. Blood Flow Metab. 25, 41–53.

Higuchi, Y., 2004. Glutathione depletion-induced chromosomal DNA fragmentation associated with apoptosis and necrosis. J. Cell. Mol. Med. 8, 455–464.

Holley, M.C., 2005. Keynote review: the auditory system, hearing loss and potential targets for drug development. Drug Discov. Today 10, 1269–1282.

Holtz, W.A., O'Malley, K.L., 2003. Parkinsonian mimetics induce aspects of unfolded protein response in death of dopaminergic neurons. J. Biol. Chem. 278, 19367–19377.

Hoya, N., Okamoto, Y., Kamiya, K., Fujii, M., Matsunaga, T., 2004. A novel animal model of acute cochlear mitochondrial dysfunction. Neuroreport 15, 1597–1600.

Kamiya, K., Fujinami, Y., Hoya, N., Okamoto, Y., Kouike, H., Komatsuzaki, R., Kusano, R., Nakagawa, S., Satoh, H., Fujii, M., Matsunaga, T., 2007. Mesenchymal stem cell transplantation accelerates hearing recovery through the repair of injured cochlear fibrocytes. Am. J. Pathol. 171, 214–226.

Kaufman, R.J., 1999. Stress signaling from the lumen of the endoplasmic reticulum: coordination of gene transcriptional and translational controls. Genes Dev. 13, 1211–1233.

Kelley, M.W., 2006. Regulation of cell fate in the sensory epithelia of the inner ear. Nat. Rev. Neurosci. 7, 837–849.

Lee, W.T., Yin, H.S., Shen, Y.Z., 2002. The mechanisms of neuronal death produced by mitochondrial toxin 3-nitropropionic acid: the roles of N-methyl-D-aspantate glutamate receptors and mitochondrial calcium overload. Neuroscience 112, 707–716.

Matsumoto, M., Minami, M., Takeda, K., Sakao, Y., Akira, S., 1996. Ectopic expression of CHOP (GADD153) induces apoptosis in M1 myeloblastic leukemia cells. FEBS Lett. 395, 143–147.

Maytin, E.V., Ubeda, M., Lin, J.C., Habener, J.F., 2001. Stress-inducible transcription factor CHOP/gadd153 induces apoptosis in mammalian cells via p38 kinase-dependent and -independent mechanisms. Exp. Cell Res. 267, 193–204.

Minowa, O., Ikeda, K., Sugitani, Y., Oshima, T., Nakai, S., Katoni, Y., Suzuki, M., Furukawa, M., Kawase, T., Zheng, Y., Ogura, M., Asada, Y., Watanabe, K., Yamanaka, H., Gotoh, S., Nishi-Takeshima, M., Sugimoto, T., Kikuchi, T., Takasaka, T., Noda, T., 1999. Altered cochlear fibrocytes in a mouse model of DFN3 nonsyndromic deafness. Science 285, 1408–1411.

Mizutari, K., Matsunaga, T., Kamiya, K., Fujinami, Y., Fujii, M., Ogawa, K., 2008. Caspase inhibitor facilitates recovery of hearing by protecting the cochlear lateral wall from acute cochlear mitochondrial dysfunction. J. Neurosci. Res. 86, 215–222.

Moisoi, N., Klupsch, K., Fedele, V., East, P., Sharma, S., Renton, A., Plun-Favreau, H., Edwards, R.E., Teismann, P., Esposti, M.D., Morrison, A.D., Wood, N.W., Downward, J., Martins, L.M., 2009. Mitochondrial dysfunction triggered by loss of HtrA2 results in the activation of a brain-specific transcriptional stress response. Cell Death Differ. 16, 449–464.

Mutai, H., Nagashima, R., Fujii, M., Matsunaga, T., 2009. Mitotic activity and specification of fibrocyte subtypes in the developing rat cochlear lateral wall. Neuroscience 163, 1255–1263.

Ohoka, N., Yoshii, S., Hattori, T., Onozaki, K., Hayashi, H., 2005. TRB3, a novel ER stress-inducible gene, is induced via ATF4-CHOP pathway and is involved in cell death. Embo J. 24, 1243–1255.

Okamoto, Y., Hoya, N., Kamiya, K., Fujii, M., Ogawa, K., Matsunaga, T., 2005. Permanent threshold shift caused by acute cochlear mitochondrial dysfunction is primarily mediated by degeneration of the lateral wall of the cochlea. Audiol. Neurootol. 10, 220–233.

Oyadomari, S., Mori, M., 2004. Roles of CHOP/GADD153 in endoplasmic reticulum stress. Cell Death Differ. 11, 381–389.

Pang, Z., Geddes, J.W., 1997. Mechanisms of cell death induced by the mitochondrial toxin 3-nitropropionic acid: acute excitotoxic necrosis and delayed apoptosis. J. Neurosci. 17, 3064–3073.

Puthalakath, H., O'Reilly, L.A., Gunn, P., Lee, L., Kelly, P.N., Huntington, N.D., Hughes, P.D., Michalak, E.M., McKimm-Breschkin, J., Motoyama, N., Gotoh, T., Akira, S., Bouillet, P., Strasser, A., 2007. ER stress triggers apoptosis by activating BH3-only protein Bim. Cell 129, 1337–1349.

Rosenstock, T.R., Carvalho, A.C., Jurkiewicz, A., Frussa-Filho, R., Smaili, S.S., 2004. Mitochondrial calcium, oxidative stress and apoptosis in a neurodegenerative disease model induced by 3-nitropropionic acid. J. Neurochem. 88, 1220–1228.

Sato, S., Gobbel, G.T., Honkaniemi, J., Li, Y., Kondo, T., Murakamii, K., Sato, M., Copin, J.C., Chan, P.H., 1997. Apoptosis in the striatum of rats following intraperitoneal injection of 3-nitropropionic acid. Brain Res. 745, 343–347.

Schulte, B.A., Adams, J.C., 1989. Distribution of immunoreactive Na+, K+-ATPase in gerbil cochlea. J. Histochem. Cytochem. 37, 127–134.

Schulte, B.A., Steel, K.P., 1994. Expression of alpha and beta subunit isoforms of Na, K-ATPase in the mouse inner ear and changes with mutations at the W/w on Sld loci. Hear. Res. 78, 65–76.

Sok, J., Wang, X.Z., Batchvarova, N., Kuroda, M., Harding, H., Ron, D., 1999. CHOP-dependent stress-inducible expression of a novel form of carbonic anhydrase VI. Mol. Cell. Biol. 19, 495–504.

Spicer, S.S., Schulte, B.A., 1996. The fine structure of spiral ligament cells relates to ion return to the stria and varies with place-frequency. Hear. Res. 100, 80–100.

Spicer, S.S., Schulte, B.A., 1998. Evidence for a medial K^+ recycling pathway from inner hair cells. Hear. Res. 118, 1–12.

Spicer, S.S., Schulte, B.A., 2002. Spiral ligament pathology in quiet-aged gerbils. Hear. Res. 172, 172–185.

Tajiri, S., Oyadomari, S., Yano, S., Morioka, M., Gotoh, T., Hamada, J.I., Ushio, Y., Mori, M., 2004. Ischemia-induced neuronal cell death is mediated by the endoplasmic reticulum stress pathway involving CHOP. Cell Death Differ. 11, 403–415.

Tanaka, K., Tomisato, W., Hoshino, T., Ishihara, T., Namba, T., Aburaya, M., Katsu, T., Suzuki, K., Tsutsumi, S., Mizushima, T., 2005. Involvement of intracellular Ca^{2+} levels in nonsteroidal anti-inflammatory drug-induced apoptosis. J. Biol. Chem. 280, 31059–31067.

Wang, X.Z., Kuroda, M., Sok, J., Batchvarova, N., Kimmel, R., Chung, P., Zinszner, H., Ron, D., 1998. Identification of novel stress-induced genes downstream of chop. EMBO J. 17, 3619–3630.

Wang, Y., Hirose, K., Liberman, M.C., 2002. Dynamics of noise-induced cellular injury and repair in the mouse cochlea. J. Assoc. Res. Otolaryngol. 3, 248–268.

Xu, C., Bailly-Maitre, B., Reed, J.C., 2005. Endoplasmic reticulum stress: cell life and death decisions. J. Clin. Invest. 115, 2656–2664.

Yu, Z., Luo, H., Fu, W., Mattson, M.P., 1999. The endoplasmic reticulum stress-responsive protein GRP78 protects neurons against excitotoxicity and apoptosis: suppression of oxidative stress and stabilization of calcium homeostasis. Exp. Neurol. 155, 302–314.

Zhao, Q., Wang, J., Levichkin, I.V., Stasinopoulos, S., Ryan, M.T., Hoogenraad, N.J., 2002. A mitochondrial specific stress response in mammalian cells. EMBO J. 21, 4411–4419.

Zinszner, H., Kuroda, M., Wang, X., Batchvarova, N., Lightfoot, R.T., Remotti, H., Stevens, J.L., Ron, D., 1998. CHOP is implicated in programmed cell death in response to impaired function of the endoplasmic reticulum. Genes Dev. 12, 982–995.

Acta Oto-Laryngologica, 2010; Early Online, 1–6

informa
healthcare

ORIGINAL ARTICLE

Vestibular function of patients with profound deafness related to *GJB2* mutation

MISATO KASAI[1], CHIERI HAYASHI[1], TAKASHI IIZUKA[1], AYAKO INOSHITA[1], KAZUSAKU KAMIYA[1], HIROKO OKADA[1], YUKINORI NAKAJIMA[1], KIMITAKA KAGA[2] AND KATSUHISA IKEDA[1]

[1]*Department of Otorhinolaryngology, Juntendo University School of Medicine, Tokyo and* [2]*National Institute of Sensory Organs, National Tokyo Medical Center, Tokyo, Japan*

Abstract

Conclusion: GJB2 mutations are responsible not only for deafness but also for the occurrence of vestibular dysfunction. However, vestibular dysfunction tends to be unilateral and less severe in comparison with that of bilateral deafness. *Objectives:* The correlation between the cochlear and vestibular end-organs suggests that some children with congenital deafness may have vestibular impairments. On the other hand, *GJB2* gene mutations are the most common cause of nonsyndromic deafness. The vestibular function of patients with congenital deafness (CD), which is related to *GJB2* gene mutation, remains to be elucidated. The purpose of this study was to analyze the relationship between *GJB2* gene mutation and vestibular dysfunction in adults with CD. *Methods:* A total of 31 subjects, including 10 healthy volunteers and 21 patients with CD, were enrolled in the study. A hearing test and genetic analysis were performed. The vestibular evoked myogenic potentials (VEMPs) were measured and a caloric test was performed to assess the vestibular function. The percentage of vestibular dysfunction was then statistically analyzed. *Results:* The hearing level of all CD patients demonstrated a severe to profound impairment. In seven CD patients, their hearing impairment was related to *GJB2* mutation. Five of the seven patients with CD related to *GJB2* mutation demonstrated abnormalities in one or both of the two tests. The percentage of vestibular dysfunction of the patients with CD related to *GJB2* mutation was statistically higher than in patients with CD unrelated to *GJB2* mutation and in healthy controls.

Keywords: *Vestibular evoked myogenic potentials, caloric test*

Introduction

Since a correlation between the peripheral auditory and vestibular systems has been identified both anatomically and phylogenetically, a subgroup of children with congenital deafness (CD) may be associated with vestibular and balance impairments [1–3]. Interestingly, the vestibular disturbance in these children gradually disappears as they grow up, probably because of a compensatory mechanism of the central nervous system. However, there have been only a few reports that conducted a detailed analysis of the vestibular function in adults with CD.

CD has been reported in approximately one child per 1000 births [1]. In more than half of these cases, the disease is caused by gene mutation. In particular, mutation in the *GJB2* gene, which encodes Cx26 in the gap junction, is known to be a most common cause (up to 50% of such cases) [2,3]. Gap junction channels enable the neighboring cells to exchange small signaling molecules. Immunohistochemical studies have revealed that Cx26 exists not only in the cochlea but also in the vestibular organs [4]. K^+ cycling involving gap junction protein Cx26 in the vestibular labyrinth, which is similar to that in the cochlea, is thought to play a fundamental role in the endolymph homeostasis and sensory transduction [5]. These findings suggest that mutations in the *GJB2* gene may thus cause vestibular dysfunction.

Correspondence: Katsuhisa Ikeda MD PhD, 2-1-1 Hongo, Bunkyoku, Tokyo 113-8421, Japan. E-mail: ike@juntendo.ac.jp

(Received 18 October 2009; accepted 30 November 2009)

ISSN 0001-6489 print/ISSN 1651-2251 online
DOI: 10.3109/00016481003596508